Target-oriented wave-equation inversion: Regularization in the reflection angle

Alejandro A. Valenciano

ABSTRACT

A complex velocity model produces shadow zones in an image due to focusing and defocusing of the seismic waves, and limited recording geometry. These shadow zones contain weak signal masked by artifacts. To recover the real signal, and reduce artifacts is necessary to go beyond migration. One option is to use a wave-equation target-oriented inversion scheme that explicitly computes the least squares inversion Hessian. The wave-equation target-oriented inversion has a big null space. It seeks to form an image where there is lack or very little data information. In this situation is where *a priori* information in the form of model regularization can help to stabilize the results. One choice for regularization, that makes physical sense, is to force the inverse image to be smooth with the reflection angle. It works by spreading the image from well illuminated to poorly illuminated reflection angles. In order to impose this smoothness constraint I implemented a chain of the subsurface-offset Hessian and a slant-stack (reflection angle to subsurface-offset) operator. Results on the Sigsbee synthetic model show that the inversion regularized in the reflection angle reduces the effect of the uneven illumination not only in the angle gathers but also in the stack image.

INTRODUCTION

Conventional imaging techniques such as migration cannot provide an accurate picture of poorly illuminated areas (Clapp, 2005). In such areas, migration artifacts or multiples can easily obscure the small amount of signal that exists, making difficult to obtain correct positioned reflectors with useful amplitudes. One reason that makes the structural image and the amplitudes unreliable in this areas is the different amount of energy illuminating the target reflectors at different angles. This is a consequence of the complexity of the subsurface and the limited acquisition geometry of the seismic experiment.

One way to improve the estimates of subsurface-acoustic properties is to use inversion (Tarantola, 1987). A linear version linking the reflectivity to the data has being applied to solve imaging problems (Nemeth et al., 1999; Kuhl and Sacchi, 2003; Clapp, 2005). This procedure computes an image by convolving the migration result with the inverse of the Hessian matrix. When the dimensions of the problem

get large, the explicit calculation of the Hessian matrix and its inverse becomes unfeasible. That is why Valenciano and Biondi (2004) and Valenciano et al. (2006) proposed the following approximations: (1) to compute the one-way wave equation Green functions from the surface to the target (or vice versa); (2) to compute an approximate Hessian, exploiting its sparse structure; and (3) to compute the inverse image following an iterative inversion scheme. The last item renders unnecessary an explicit computation of the inverse of the Hessian matrix.

The wave-equation inversion problem has a big null space. That is why a model regularization needs to be added. Two different regularization schemes for wave-equation inversion have been discussed in the literature. First, a geophysical regularization which penalizes the roughness of the image in the offset-ray-parameter dimension (which is equivalent the reflection-angle dimension) (Prucha et al., 2000; Kuhl and Sacchi, 2003). Second, a differential semblance operator to penalize the energy in the image not focused at zero subsurface-offset (Shen et al., 2003; Valenciano, 2006, 2007).

In this paper I study the regularization in the reflection angle of the target-oriented wave-equation inversion. That choice for the regularization forces the inverse image to be smooth with the reflection angle. It works by spreading the image from well illuminated to poorly illuminated reflection angles. In order to impose this smoothness constraint I implemented a chain of the subsurface-offset Hessian and a slant-stack (reflection-angle to subsurface-offset) operator. I used the Sigsbee synthetic model to validate the methodology, showing that the inversion reduces the effect of the uneven illumination in the angle gathers and in the angle stack.

TARGET-ORIENTED WAVE-EQUATION INVERSION

Linear least-squares inversion

Tarantola (1987) formalizes the geophysical inverse problem. A linear version linking the reflectivity to the data has being discuss in the literature (Nemeth et al., 1999; Kuhl and Sacchi, 2003; Clapp, 2005). It provides a theoretical approach to compensate for experimental deficiencies (e.g., acquisition geometry, complex overburden), while being consistent with the acquired data. This approach can be summarized as follows: given a linear modeling operator $\mathbf{L}$, compute synthetic data $\mathbf{d}$ using $\mathbf{d} = \mathbf{L}\mathbf{m}$ where $\mathbf{m}$ is a reflectivity model. Given the recorded data $\mathbf{d}_{obs}$, a quadratic cost function,

$$S(\mathbf{m}) = \|\mathbf{d} - \mathbf{d}_{obs}\|^2 = \|\mathbf{L}\mathbf{m} - \mathbf{d}_{obs}\|^2, \tag{1}$$

is formed. The reflectivity model $\hat{\mathbf{m}}$ that minimizes $S(\mathbf{m})$ is given by the following:

$$\hat{\mathbf{m}} = (\mathbf{L}'\mathbf{L})^{-1}\mathbf{L}'\mathbf{d}_{obs} = \mathbf{H}^{-1}\mathbf{m}_{mig}, \tag{2}$$

where $\mathbf{L}'$ (migration operator) is the adjoint of the linear modeling operator $\mathbf{L}$, $\mathbf{m}_{mig}$ is the migration image, and $\mathbf{H} = \mathbf{L}'\mathbf{L}$ is the Hessian of $S(\mathbf{m})$.

The main difficulty with this approach is the explicit calculation of the inverse Hessian. In practice, it is more feasible to compute the least-squares inverse image as the solution of the linear system,

$$\mathbf{H}\hat{\mathbf{m}} = \mathbf{m}_{mig}, \tag{3}$$

by using an iterative inversion algorithm.

Regularization in the reflection angle

Equation 3 can be solved in different domains: poststack image domain (zero subsurface-offset) (Valenciano et al., 2006), prestack subsurface-offset image domain (Valenciano, 2006, 2007), or prestack reflection-angle image domain (this paper). Valenciano (2007) shows that a prestack regularization is necessary to reduce the noise in the result without smoothing the image space.

In this paper I discuss the use of the regularization in the reflection-angle domain (Prucha et al., 2000; Kuhl and Sacchi, 2003). The regularization operator is a derivative in the reflection-angle dimension that penalizes the roughness of the image. It works by spreading the image from well illuminated to poorly illuminated reflection angles.

The general fitting goals corresponding to the angle-domain inversion are:

$$\begin{aligned} \mathbf{H}(\mathbf{x},\mathbf{h};\mathbf{x}',\mathbf{h}')\mathbf{S}_{\Theta\rightarrow\mathbf{h}}\hat{\mathbf{m}}(\mathbf{x},\Theta) - \mathbf{m}_{mig}(\mathbf{x},\mathbf{h}) &\approx 0, \\ \varepsilon\mathbf{D}_{\Theta}\hat{\mathbf{m}}(\mathbf{x},\Theta) &\approx 0, \end{aligned} \tag{4}$$

where $\mathbf{H}(\mathbf{x},\mathbf{h};\mathbf{x}',\mathbf{h}')$ is the subsurface-offset Hessian (Valenciano, 2006), $\mathbf{S}_{\Theta\rightarrow\mathbf{h}}$ is a slant-stack operator that transforms the image from angle to subsurface-offset domain, $\mathbf{D}_{\Theta}$ is a derivative operator, $\mathbf{x} = (z, x, y)$ is a point in the image, $\mathbf{h} = (h_x, h_y, h_z)$ is the half subsurface-offset, and $\Theta = (\gamma, \theta)$ reflection, and azimuth angle.

In the next section I discuss on the numerical solution of the inversion problem stated in equation 4 applied to the imaging of Sigsbee model. Notice that in this paper I use a 2D example where only the h_x component of the subsurface-offset and the reflection-angle γ are used.

NUMERICAL RESULTS: SIGSBEE MODEL

The Sigsbee data set was modeled by simulating the geological setting found on the Sigsbee escarpment in the deep-water Gulf of Mexico. The model exhibits the illumination problems due to the complex salt shape, characterized by a rugose salt top (see Figure 1). Figure 2 shows the shot-profile migration image (using cross-correlation imaging condition) corresponding to the portion of Sigsbee model shown in figure 1. Notice how the amplitudes of the reflectors fade away as they get closer to the salt.

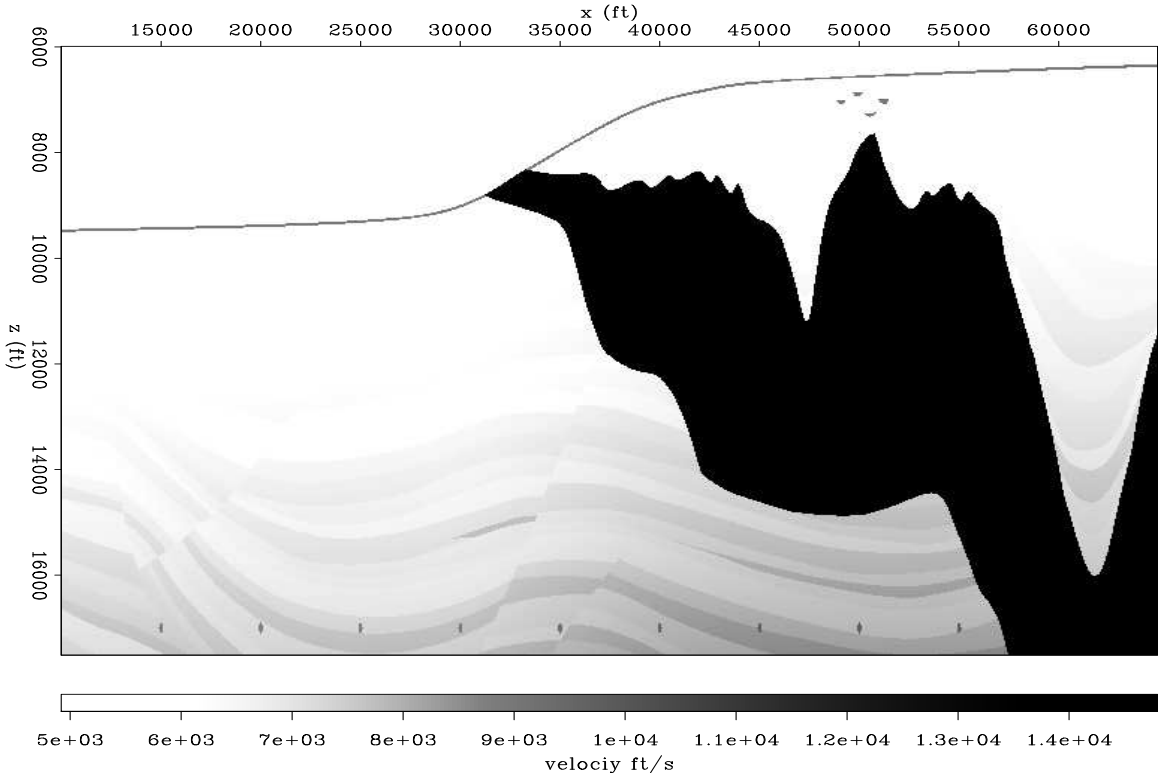

Figure 1: Sigsbee stratigraphic velocity model.

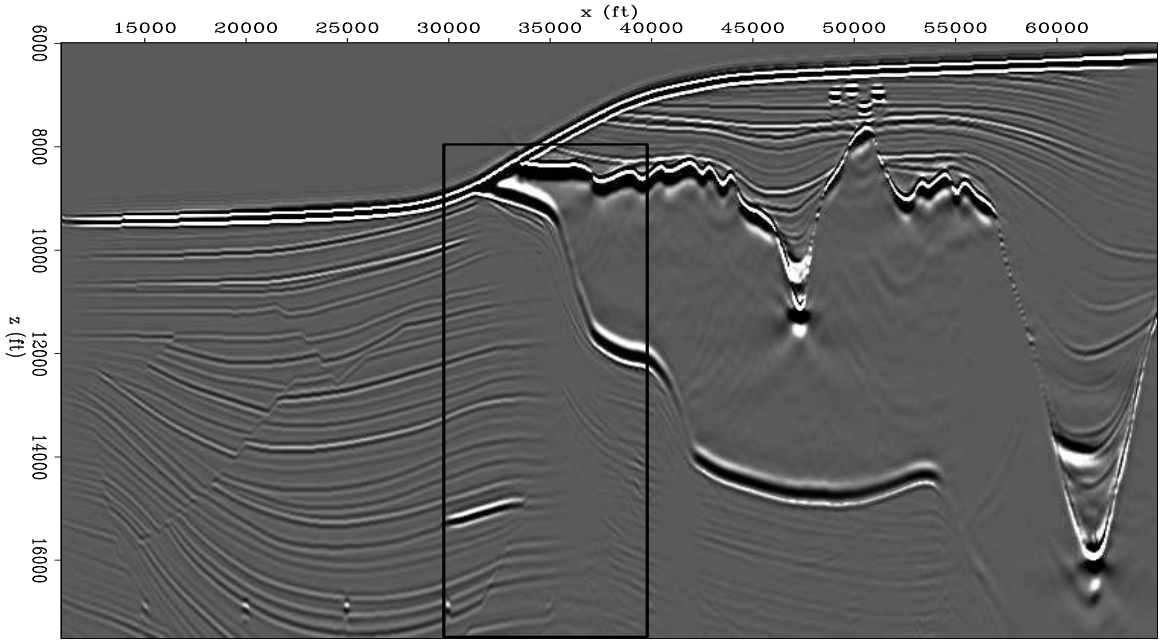

Figure 2: Sigsbee shot-profile zero subsurface-offset migration image using cross-correlation imaging condition. The velocity model corresponds to Figure 1

I choose a target zone close to the salt to evaluate the effects of illumination on imaging (rectangle in Figure 2). A good picture of the complexity of the focusing and defocusing of the seismic energy in this model is given by Figure 3, which shows the diagonal of the Hessian matrix in the target zone. Light gray correspond to hight amplitude and dark gray to low amplitudes. Notice how the concave and convex shape of the base of the salt, respectively, focus and defocus the seismic energy as waves propagate trough the medium.

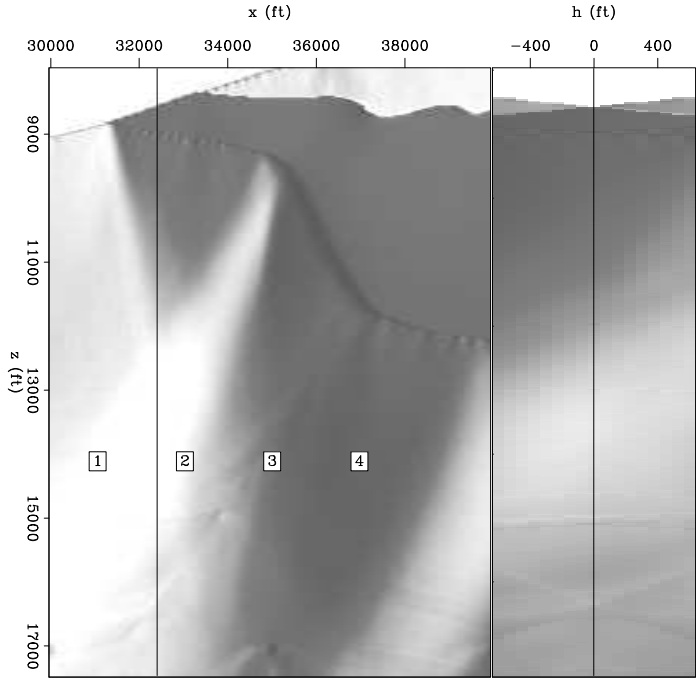

Figure 3: Diagonal of the target-oriented Hessian matrix. White correspond to hight amplitude

Four rows of the target-oriented Hessian matrix are shown in Figure 4. They are $11 \times 21 \times 17$ coefficient filter for constant depth and constant subsurface-offset ($h_x = 0\,ft$) at four different x coordinates (from the sediments to the salt boundary Figure 3). Notice that only the elements of the matrix corresponding to one side of the diagonal are shown. Since the Hessian matrix is symmetric by definition half of the off diagonal terms are not computed. Figure 4a shows point 1, with coordinates $\mathbf{x} = (14000, 31000)\,ft$ (far from the salt). Figure 4b shows point 2, with coordinates $\mathbf{x} = (14000, 33000)\,ft$. Figure 4c shows point 3, with coordinates $\mathbf{x} = (14000, 35000)\,ft$. Figure 4d shows point 4, with coordinates $\mathbf{x} = (14000, 37000)\,ft$. The shape of the filter is not dependent only on the acquisition geometry but the subsurface geometry (presence of the salt body). In the area less affected by the salt the energy is concentrated around the diagonal (center of the filter), but as we get closer to the salt, the illumination varies (in intensity and angle) and the filter behaves differently. This is due to a focusing and defocusing effect created by the salt. To correct this effect we computed the least-squares inverse image.

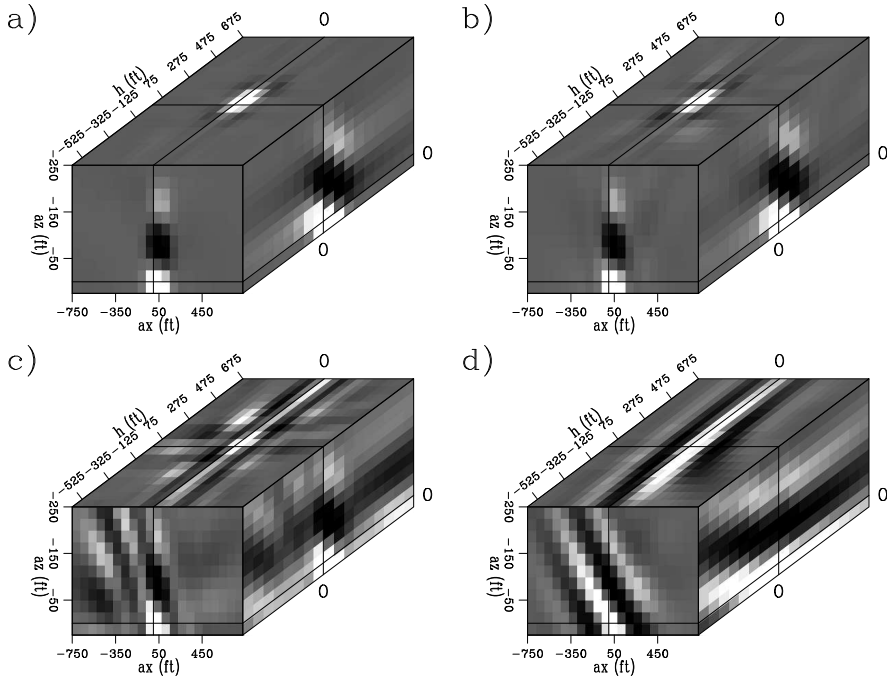

Figure 4: Four rows of the target-oriented Hessian matrix, (a) point 1 $\mathbf{x} = (14000, 31000)\, ft$, (b) point 2 $\mathbf{x} = (14000, 33000)\, ft$, (c) point 3 $\mathbf{x} = (14000, 35000)\, ft$, and (d) point 4 $\mathbf{x} = (14000, 37000)\, ft$.

Postack comparison

Figure 5 shows the reflection coefficients, and the zero subsurface-offset migration. The zero subsurface-offset inversion (Valenciano et al., 2006), and the stack of the inversion with regularization in the reflection angle can be seen in Figure 6. In the migration result shown in Figure 5b the reflectors dim out in the areas of low illumination (see left panel of Figure 3 for reference). In contrast, the zero subsurface-offset inversion (Figure 6a) and the stack of the inversion with regularization in the reflection angle (Figure 6b) show that: the reflectors can be followed into the shadow zones with the correct kinematics, the resolution increases, the footprint of the irregular illumination is diminished, and the faults can be followed and interpreted closer to the salt body.

It is important to remark the differences between the two inversion results in Figure 6a and Figure 6b. The inversion with regularization in the reflection angle has better defined fault planes and sediments more accurately extended into the shadow zones than the zero subsurface-offset inversion. Also, the level of noise in the zero subsurface-offset inversion is much higher. This is due to the fact that no regularization was applied in the zero subsurface-offset inversion. The regularization in the reflection angle helps to spread the image from well illuminated to poorly illuminated reflection angles, reducing the noise and eliminating non consistent artifacts.

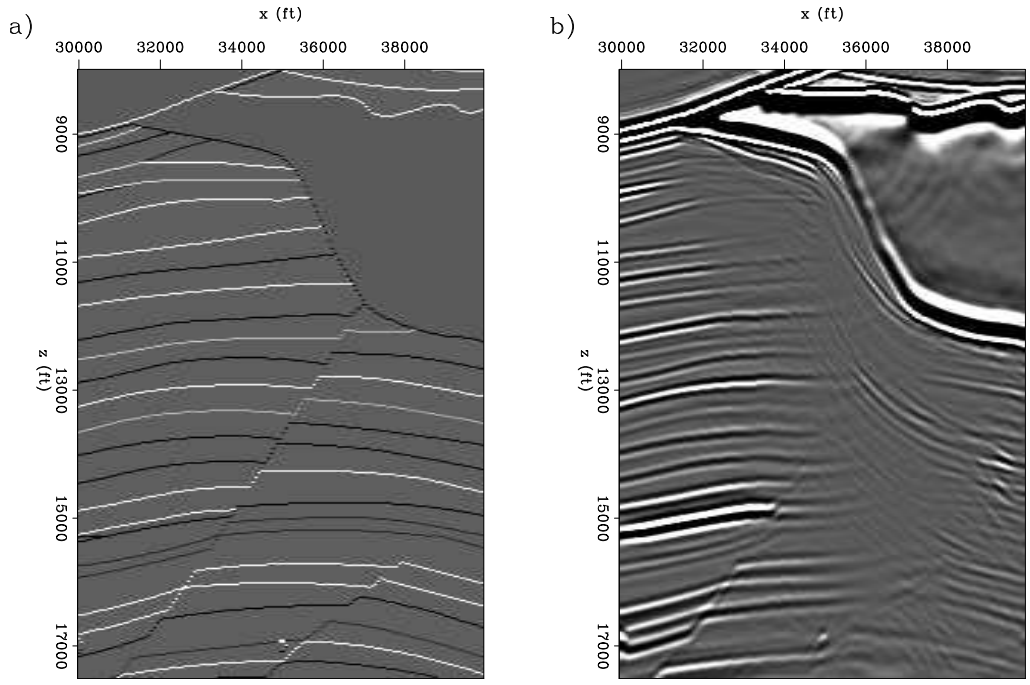

Figure 5: Target area comparison. (a) reflection coefficients, and (b) zero subsurface-offset migration.

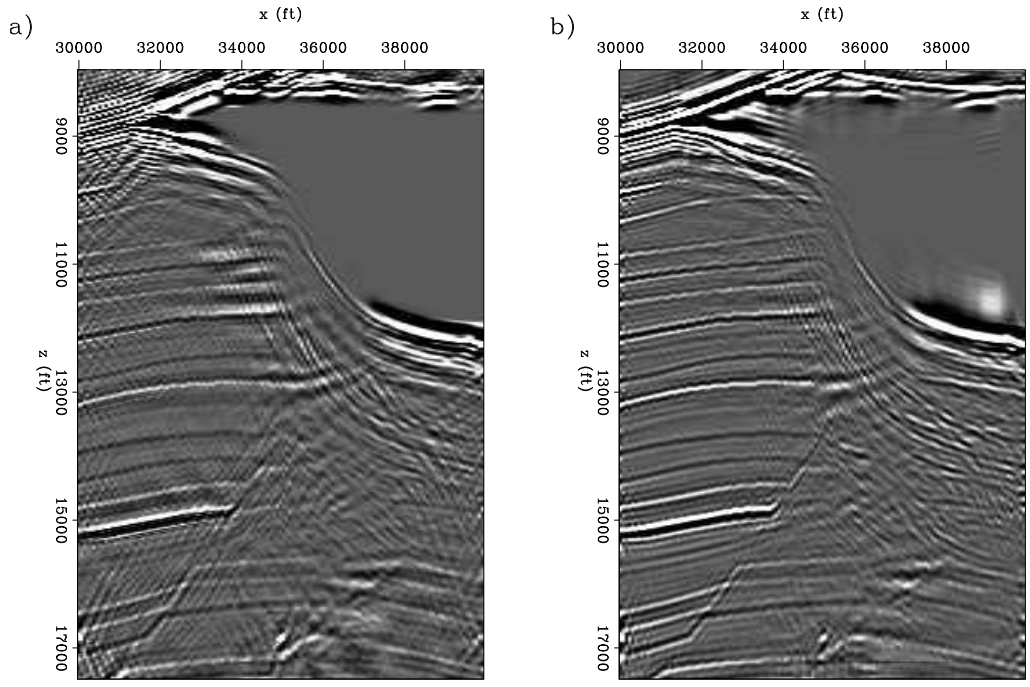

Figure 6: Target area comparison. (a) zero subsurface-offset inversion, and (b) stack of the inversion with regularization in the reflection angle (zero subsurface-offset).

The salt in the inversion images looks distorted because a residual weight designed to decrease the salt contribution was used (data values in the salt boundary are bigger than everywhere else Figure 2). This was necessary to avoid the solver expending most of the iterations decreasing the residuals in that area.

Prestack comparison

Figures 7 and 8 show the migration result in the subsurface-offset domain and the reflection-angle domain, respectively. The migration in the subsurface-offset domain is the "data", and corresponds to the right hand side of equation 4. The migration at the reflection-angle domain is shown for comparison purposes, since the model space corresponds to the reflection-angle domain.

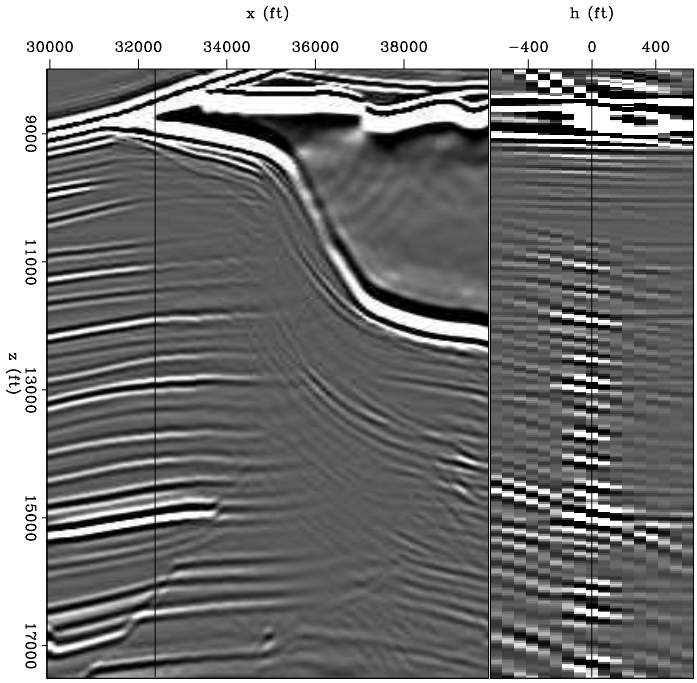

Figure 7: Sigsbee shot-profile migration(subsurface-offset) using cross-correlation imaging condition.

Figures 9 and 10 show the inversion without and with regularization in the reflection-angle domain, respectively (compare to migration in Figure 8). The left panel shows a common angle section (24°). The migration shows a big shadow zone below the salt (Figure 8). In the inversion without regularization (Figure 9) the shadow zone has been filled partially but the results are very noisy. The regularized inversion image (Figure 10) gives a better result, less noisy and with some of the reflectors extended into the shadow zone.

If we look in more detail into the angle gathers (Figures 11, 12, and 13) the effect of the inversion and the regularization can be understood separately. Figure 11 shows

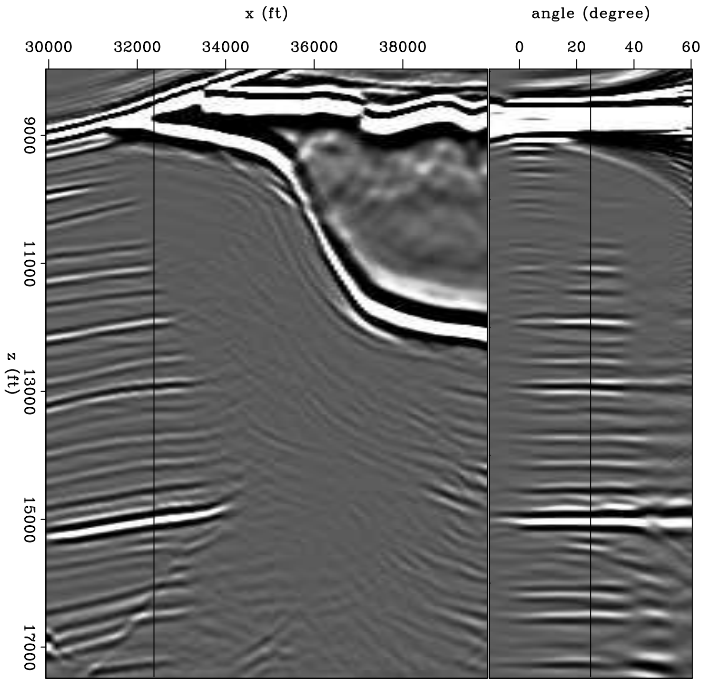

Figure 8: Sigsbee shot-profile migration (reflection angle) using cross-correlation imaging condition.

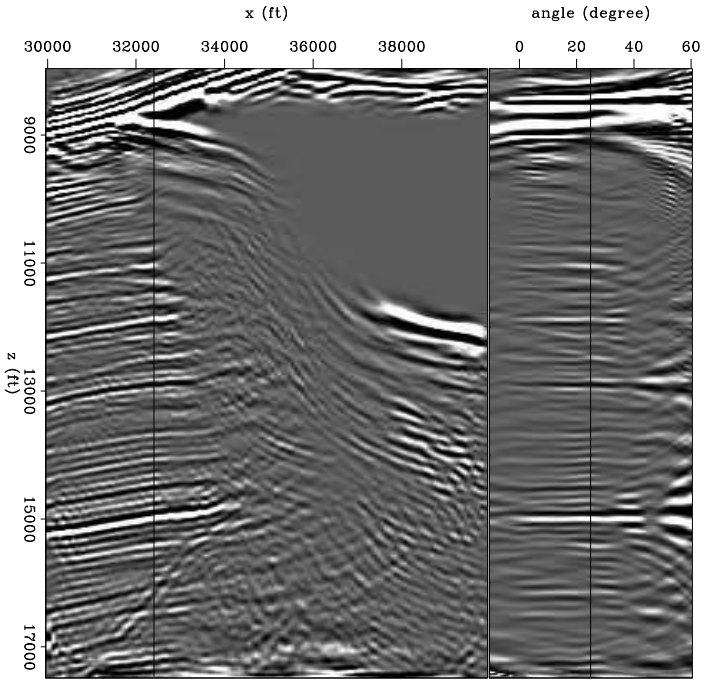

Figure 9: Sigsbee inversion without regularization (reflection angle).

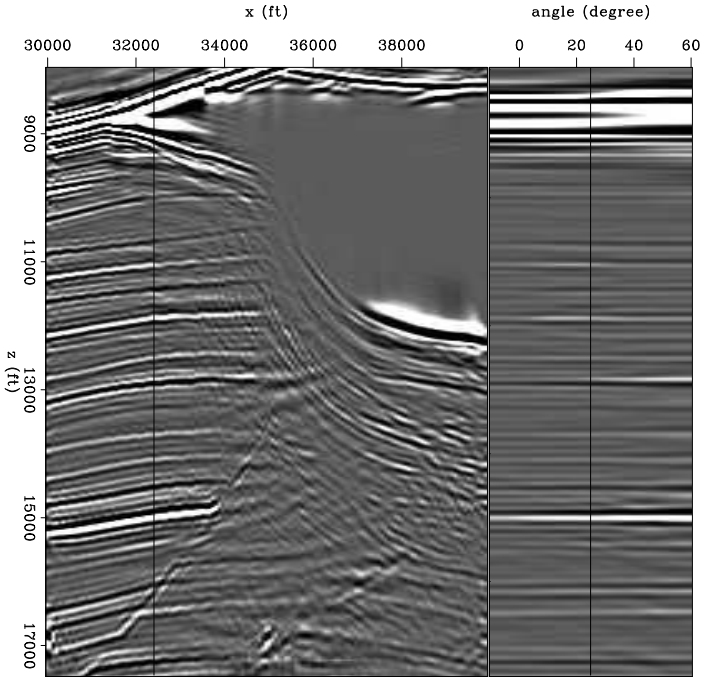

Figure 10: Sigsbee inversion with regularization (reflection angle).

angle gathers at three different x coordinate positions $x = 32300\,ft$, $x = 33700\,ft$, $x = 35700\,ft$. Notice the holes in some of the reflectors, also notice that there are salt related multiple reflections (non-flat events in the angle gathers). After inversion without regularization (Figure 12) some the wholes have being filled but the noise has increase as well as the bandlimited related artifacts off the slant-stack, also the multiples had been increased in amplitude. The inversion with regularization (Figure 13), gives the best result. The wholes have being filled, the noise is reduced, and the far-angle-multiple energy is decreased.

CONCLUSIONS

The target-oriented wave-equation inversion, regularized in the reflection angle, reduces the effect of the uneven illumination not only in the angle gathers but also in the stack image. It gives better results than the zero subsurface-offset inversion (Valenciano et al., 2006) because the regularization helps to spread the image from well illuminated to poorly illuminated reflection angles, reducing the noise and eliminating non consistent artifacts. Results in Sigsbee data set show that even with very complex subsalt illumination the inversion can give a good image.

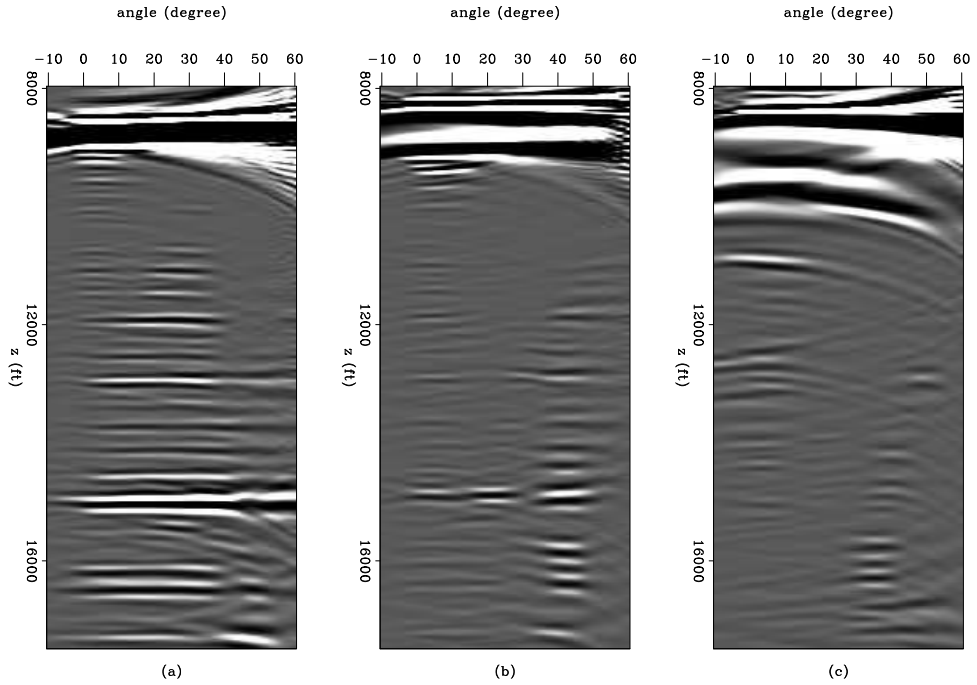

Figure 11: Sigsbee migration (reflection angle). Angle gathers at three different x coordinate positions (a) $x = 32300\,ft$, (b) $x = 33700\,ft$, and (c) $x = 35700\,ft$

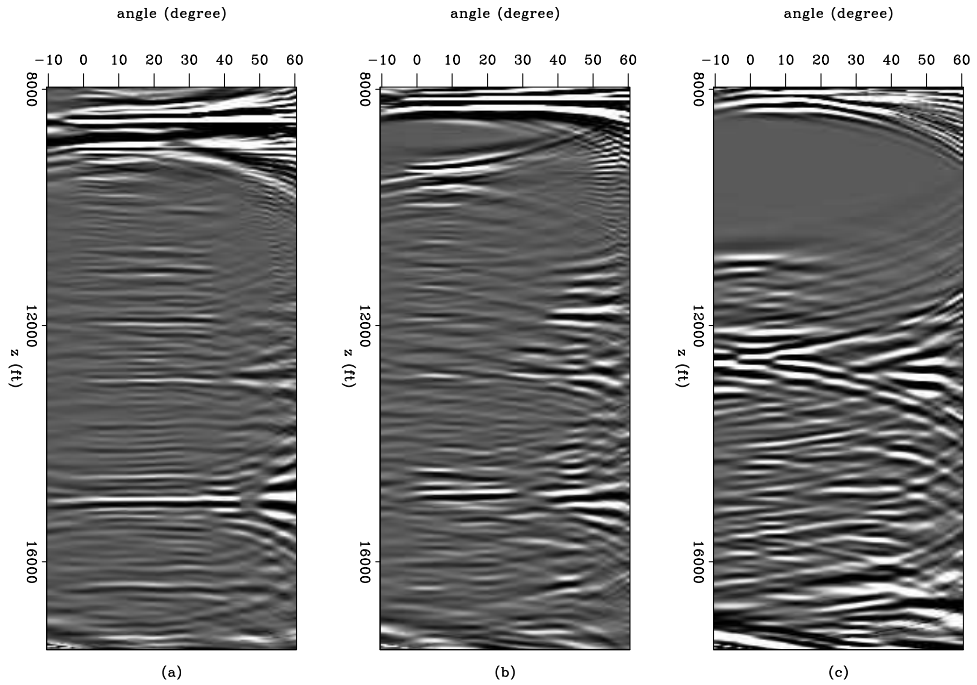

Figure 12: Sigsbee inversion without regularization (reflection angle). Angle gathers at three different x coordinate positions (a) $x = 32300\,ft$, (b) $x = 33700\,ft$, and (c) $x = 35700\,ft$

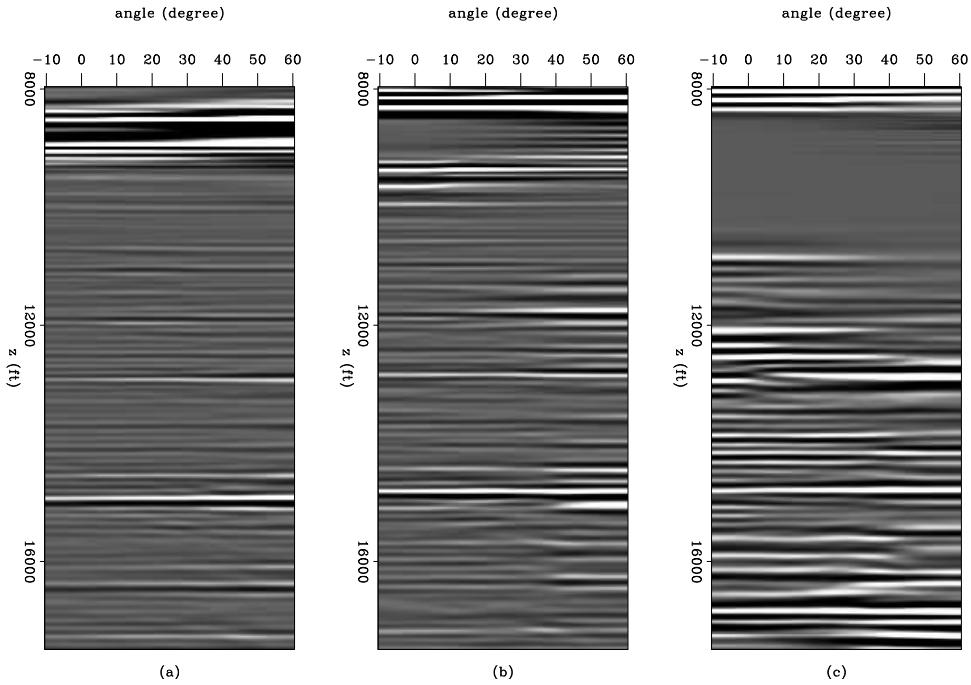

Figure 13: Sigsbee inversion with regularization (reflection angle). Angle gathers at three different x coordinate positions (a) $x = 32300\,ft$, (b) $x = 33700\,ft$, and (c) $x = 35700\,ft$

ACKNOWLEDGMENTS

I would like to thank the SMAART JV for the synthetic data used in the experiments, as well as the Stanford Exploration Project sponsors for financial and technical support.

REFERENCES

Clapp, M. L., 2005, Imaging under salt: illumination compensation by regularized inversion: PhD thesis, Stanford University.

Kuhl, H. and M. D. Sacchi, 2003, Least-squares wave-equation migration for AVP/AVA inversion: Geophysics, **68**, 262–273.

Nemeth, T., C. Wu, and G. T. Schuster, 1999, Least-squares migration of incomplete reflection data: Geophysics, **64**, 208–221.

Prucha, M. L., R. G. Clapp, and B. Biondi, 2000, Seismic image regularization in the reflection angle domain: SEP-Report, **103**, 109–119.

Shen, P., W. Symes, and C. C. Stolk, 2003, Differential semblance velocity analysis by wave-equation migration: 73st Annual International Meeting, SEG, Expanded Abstracts, Expanded Abstracts, 2132–2135.

Tarantola, A., 1987, Inverse problem theory: Methods for data fitting and model parameter estimation: Elsevier Science Publication Company, Inc.

Valenciano, A. A., 2006, Target-oriented wave-equation inversion with regularization in the subsurface offset domain: SEP-Report, **124**, 85–94.

———, 2007, Target-oriented wave-equation inversion: Sigsbee model: SEP-Report, **129**, 65–74.

Valenciano, A. A. and B. Biondi, 2004, Target-oriented computation of the wave-equation imaging Hessian: SEP-Report, **117**, 63–76.

Valenciano, A. A., B. Biondi, and A. Guitton, 2006, Target-oriented wave-equation inversion: Geophysics, **71**, A35–A38.